

REVIEW ARTICLE



Industry Research

Translating digital anthropometry measurements obtained from different 3D body image scanners

Nicholas Ashby¹, G. Jake LaPorte¹, Daniel Richardson¹, Michael Scioletti¹, Steven B. Heymsfield², John A. Shepherd³, Michael McGurk⁴, Brenda Bustillos⁴, Nicholas Gist⁵ and Diana M. Thomas¹✉

This is a U.S. Government work and not under copyright protection in the US; foreign copyright protection may apply 2023

BACKGROUND: Body image scanners are used in industry and research to reliably provide a wealth of anthropometric measurements within seconds. The demonstrated utility of the scanners drives the current proliferation of more commercially available devices that rely on their own reference body sites and proprietary algorithms to output anthropometric measurements. Since each scanner relies on its own algorithms, measurements obtained from different scanners cannot directly be combined or compared.

OBJECTIVES: To develop mathematical models that translate anthropometric measurements between the three popular commercially available scanners.

METHODS: A unique database that contained 3D scanner measurements in the same individuals from three different scanners (Styku, Human Solutions, and Fit3D) was used to develop linear regression models that translate anthropometric measurements between each scanner. A limits of agreement analysis was performed between Fit3D and Styku against Human Solutions measurements and the coefficient of determination, bias, and 95% confidence interval were calculated. The models were then applied to normalized scanner data from four different studies to compare the results of a k-means cluster analysis between studies. A scree plot was used to determine the optimal number of clusters derived from each study.

RESULTS: Correlations ranged between $R^2 = 0.63$ (Styku and Human Solutions mid-thigh circumference) to $R^2 = 0.97$ (Human Solutions and Fit3D neck circumference). In general, Fit3D had better agreement with Human Solutions compared to Styku. The widest disagreement was found in chest circumference (Fit3D (bias = 2.30, 95% CI = [-3.83, 8.43]) and Styku (bias = -5.60, 95% CI = [-10.98, -0.22])). The optimal number of body shape clusters in each of the four studies was consistently 5.

CONCLUSIONS: The newly developed models that translate measurements between the scanners Styku and Fit3D to predict Human Solutions measurements make it possible to standardize data between scanners allowing for data pooling and comparison.

European Journal of Clinical Nutrition (2023) 77:872–880; <https://doi.org/10.1038/s41430-023-01289-5>

INTRODUCTION

Digital anthropometry obtained from 3D body scanners has revolutionized clothing sizing [1] and body shape tracking in the fitness industry [2]. Within seconds, the scanners obtain hundreds of anthropometric measurements, reducing the burden entailed during manual collections of measurements and providing new scientific insights. Recently, 3D body image scanners were used to predict injuries in Army basic training [3], classify body shape with body composition [4, 5], and estimate risk for metabolic disease [6].

In response to the utility of 3D body image scanners, several different scanner brands offer themselves commercially [7], however, the measurements by scanner can differ. For example, each individual scanner uses different proprietary algorithms with reference points on the body that define where and how to obtain

measurements. For this reason, scanners of different brands may output multiple different measurements for the same individual's body site.

Unfortunately, institutions using different scanners can prohibit pooling data or comparing across datasets when required. For example, recently, the US Army used the Fit3D scanner evaluate body composition and physical fitness [8]. A similar study was conducted at the United States Military Academy in 2020, but using the Styku scanner [9]. In addition, two other US military sites, Fort Jackson, and Lackland Air Force Base, obtained measurements for uniform sizing using the Human Solutions scanner [9]. The study at the United States Military Academy identified five archetype body shapes through a cluster analysis and linked these shapes to performance. However, the sample size was small and the population at the

¹Department of Mathematical Sciences, United States Military Academy, West Point, NY, USA. ²Pennington Biomedical Research Center, Baton Rouge, LA, USA. ³University of Hawai'i Cancer Center, Honolulu, HI, USA. ⁴Research and Analysis Directorate, U.S. Army Center for Initial Military Training (CIMT), U.S. Army Training & Doctrine Command (TRADOC), Fort Eustis, VA, USA. ⁵Department of Physical Education, United States Military Academy, West Point, NY, USA. ✉email: diana.thomas@westpoint.edu

Received: 23 August 2022 Revised: 31 March 2023 Accepted: 25 April 2023

Published online: 10 May 2023

United States Military Academy is not representative of the larger Army. Addressing this question with a larger more diverse military population by pooling the data from the Fit3D study or the latent data from Fort Jackson and Lackland Air Force Base was not possible since the scanners used were different.

Here, we build upon initial work [7] that used an earlier version of a unique dataset that contains digital anthropometry measurements from 109 participants captured with three commercially available 3D scanners to develop models that convert measurements from one scanner to another. The original dataset in [7] has increased since publication from $N=35$ to $N=109$ and the larger dataset provides additional data to develop the models required to translate measurements from one scanner to another.

METHODS

Study design

This study evaluated whether circumference measurements obtained at similar sites (for example the neck) but from different 3D body scanners are correlated. We achieved this methodologically through two steps.

Step 1. We first used a dataset that contained measurements of the same participants using three of the most popular commercially available scanners to develop models that convert anthropometric measurements from one scanner's scale to another. For example, all three scanners output a neck circumference measurement, however, the three measurements between scanners did not provide the same values for the measurement. Each scanner used proprietary algorithms to identify reference locations that define how and where to measure the neck circumference. In this example, we developed a model that translates all three neck circumferences to one standardized neck circumference measurement.

Step 2. The standardized measurements allowed us to compare findings across datasets. To illustrate the utility of body scanner standardization, we first tested it on several smaller and larger sized datasets. In an earlier study ($N=239$) (13), researchers used 13 anthropometric measurements obtained with the Styku device in a k -means clustering algorithm to identify five distinct clusters within the data. However, the literature (16) suggests that a larger sample size would yield even more clusters. To test whether larger sample sized data will result in additional clusters, we leveraged two larger datasets of anthropometric measurements obtained using Human Solutions. We standardized the smaller Styku datasets to Human Solutions measurement and then quantified the number of body shapes that resulted from applying a clustering algorithm to the data as sample size increased.

3D scanning devices

Common to all 3D scanners mentioned below, participants must wear form fitting clothing, so the scanner does not confuse the body's reference points with loose clothing folds. This standard practice negates operator impact on measurements.

Styku. The Styku scanner (Model S100) serves as a portable 3D body scanner designed for use in a variety of industries including fitness, sport, medicine, and physical therapy. The device consists of a circular pedestal (60 cm diameter) and a cylindrical post (25.4 cm diameter), which contains several cameras that perform the 3D body scan. Before scanning, the pedestal rests 63.5 cm away from the 117 cm tall post. Participants stand on the pedestal with their feet shoulder-width apart, arms extended away from the body, and hands balled into fists. When the scan begins, the pedestal rotates and the cameras in the post start

creating the 3D image. Styku scans take 35 seconds to complete with a measurement precision of 5 mm. The Styku scanner advertises as lightweight and portable.

Human solutions. The Human Solutions scanner (Vitus smart XXL) proceeds from the German company Vitronic. Vitronic markets 3D scanners for clothing, 3D figure creation, and performance diagnostics. The Smart XXL scanner consists of four pods, each containing a separate scanner. Human Solutions scans take 12 s to complete. Both the U.S. Army and the U.S. Air Force utilize the Vitus smart XXL for uniform sizing at initial entry training [3, 9].

Fit3D. Fit3D, Inc., an American company, produces the Fit3D ProScanner [10]. The company markets the scanner for the fitness industry. The ProScanner consists of a camera tower (180.34 cm height), turntable, and handles. An interactive touchscreen integrates on the camera tower assembly providing an interface for users to interact with the system. The first measurement captures a user's weight using the turntable's built-in scale. After recording weight, users grab both handles and make an "A-frame pose" with straight arms and legs. The turntable spins 360-degrees to generate a 3D avatar, adding it to the user's profile. The entire scan, including weight measurement, takes less than 3 min to complete. Users can disassemble and move the ProScanner as desired.

Study data

Data used to standardize 3D body shape measurements

Pennington Biomedical Research Center Study: The reference data used for this study originated from the Pennington Biomedical Research Center (PBRC) with collection occurring between January 2014 and December 2015 (Clinical Trial: NCT02118675) to compare body composition measured by bioelectrical impedance analysis (BIA), dual-energy x-ray absorptiometry (DXA), air displacement plethysmography, manual and 3D scanner measured body circumferences, as well as percent body fat derived from ultrasound measured tissue thickness. Details of the original study are published elsewhere [11]. The PBRC study compiled anthropometry measured using four different commercially available 3D scanners along with manually measurements. We restricted our analysis to three of the 3D body scanner measurements: Styku, Human Solutions, and Fit3D. We chose these scanners due to their similar marketing, wide availability, and our access to additional datasets with measurements from each. One hundred and fifty participants received scans from the three devices, specifically the Human Solutions, Styku and Fit3D devices. The PBRC study existed as the only known dataset that provides body circumference measurements from all three 3D scanners in the same participants. All participants provided informed consent and the study protocol received review and approval from the PBRC Institutional Review Board (#12021).

Data used to classify body shapes

University of Hawai'i: The University of Hawaii Cancer Center (UHCC) in Honolulu, HI formed this dataset as part of the Shape Up! study conducted in conjunction with PBRC, University of California at San Francisco, and the University of Washington [12]. Shape Up! enrolled a diverse population with equal numbers in BMI classification groups, age, and gender. The original study focused on using 2D and 3D images to predict body composition. The Shape Up! study used a Styku device to scan a total of 527 participants. We used the Styku measured circumferences in our analysis after transferring the data to a standard scale to classify total number of distinct body shapes identified through clustering.

Approval for this study's protocol authorized from three separate IRBs (PBRC, IRB study no. 2017–10, FWA no. 00006218; UH ORC, CHS no. 24282; and UCSF, IRB no. 16-20,197).

Lackland Air Force Base: Lackland Air Force Base just outside of San Antonio, TX, is the only site for the U.S. Air Force's initial recruit entry training. Between February 2011 and November 2016, 64,000 Air Force recruits were scanned for uniform sizing at Lackland using the Human Solutions' Vitus smart XXL scanner. Trained cadre supervised participants during the scan, correcting any protocol violations (i.e., incorrect pose, not removing loose clothing, etc.) before the scan executed. This element of control greatly reduced the number of measurement errors and allowed the Lackland dataset to serve as a baseline of comparison for other Human Solutions datasets [3, 9, 13]. The large sized Lackland dataset was used to determine the ceiling for the number of identifiable body shapes. The United States Military Academy Institutional Review Board (#18-020) determined this study's protocol as not constituting human subjects' research.

West point: The United States Military Academy at West Point, NY used Styku scanner measurements in a study designed to determine the relationship between body shape and performance on the new Army Combat Fitness Test (ACFT) [9]. A total of 239 cadets were scanned between February and March 2021 using the Styku S100 scanner. The anthropometric measurements represented a small cohort of relatively homogeneous individuals (ages 17–27 and determined physically fit for admission and retention at the United States Military Academy). The original study received approval from the USMA Institutional Review Board (Number CA20-009) with written informed consent obtained from all study participants.

Fort Jackson: Fort Jackson, SC serves as the largest of the four U.S. Army posts that conduct basic combat training (BCT). The Human Solutions Vitus smart XXL scanner measurements supplied for this study originally were used to determine uniform sizing. Between February and October 2017, 17,680 recruits were scanned using Human Solutions [3]. The United States Military

Academy Institutional Review Board (#18-020) determined that accessing this data for analysis did not constitute human subjects research.

Table 1 summarizes by sex, the age, height, and BMI of the participants across all studies used for the different analyses in this study.

Data pre-processing

Data pre-processing involved several key steps. The detailed workflow is demonstrated below in steps and summarized with a flowchart in Fig. 1.

Step 1: Synthesized observations scanned by all three scanners. Since we sought to develop a model that translates similar measurements across the three scanners, each observation needed corresponding measurements from the two other scanners. The Styku dataset contained 109 complete observations, while the Human Solutions and Fit3D datasets contained 107 and 108 complete observations, respectively. Therefore, retaining observations of complete shared measurements resulted in a synthesized dataset of 107 records.

Step 2: Identified the visually closest body site measurements across all three scanners. Two of the scanners, Human Solutions and Fit3D, offered multiple measurements that could visually represent a single measurement on Styku. Thus, to compile a dataset of similar measurements across the three scanners, we first determined which measurements all three scanners share. Since the Styku S100 returned the fewest number of measurements, it limited us to 13 common body circumferences sites (see Fig. 2). Using these 13 sites, we visually compared potential analogous body sites on Human Solutions and Fit3D avatars that offer corresponding measurements.

Forearm, narrowest part of the waist, and mid-thigh circumferences were available in the Fort Jackson dataset, however, the Lackland Human Solutions machine was an earlier version and did not include these measurements. To estimate the forearm circumference in the Lackland dataset, we used Fort Jackson data to calculate a "forearm factor" by first averaging the lower and upper bicep circumference (which exists in both datasets) to arrive at a bicep circumference and then calculate the ratio of the average of bicep circumference and the forearm circumference resulting in 1.15. The Fort Jackson calculated forearm factor times the Lackland average of lower and upper bicep circumference was used to arrive at a forearm estimate for the Lackland dataset. Similarly, the narrowest part of the waist circumference factor was developed by using the ratio of the average of the waist circumference at the abdomen (available in both datasets) and the average of the circumference at the narrowest part of the waist, which came out to 1.06. The narrowest part of the waist circumference was estimated in the Lackland data by multiplying 1.06 to the abdominal waist circumference. Finally, a mid-thigh factor was calculated from the Fort Jackson data by first calculating the average of the upper and lower thigh circumference (available in both datasets) and then taking the ratio of this average over the entire Fort Jackson dataset with the average of the mid-thigh circumference. This came out to 0.96. The Lackland mid-thigh circumference for each observation was then estimated as 0.96 times the average of the upper and lower thigh circumference.

We next regressed the Human Solutions measurements against Fit3D and Styku measurements. We recorded as best match the measurements from the Human Solutions and Fit3D that yielded the highest R^2 when regressed against the Styku measurements.

Step 3: Removed outliers. Scanner measurements are sensitive to participant positioning [3, 9]. Any slight movement or poor

Table 1. Participant characteristics by study.

Study Name	Lackland AFB	Hawaii	West Point
N Male (%)	23,998 (98.0%)	230 (43.6%)	156 (65.3%)
Female (%)	484 (2.0%)	297 (56.4%)	83 (34.7%)
Height (M)	175.03 ± 6.56	175.57 ± 7.89	179.44 ± 7.86
(cm) (F)	163.30 ± 6.77	161.54 ± 6.61	166.32 ± 6.68
BMI (M)	N/A	27.86 ± 6.14	25.32 ± 2.99
(kg/m ²) (F)		27.27 ± 7.77	22.36 ± 2.22
Age (M)	N/A	45.03 ± 16.62	N/A
(F)		47.23 ± 16.35	
Study Name	Fort Jackson	PBRC	
N Male (%)	14,080 (74.4%)	42 (38.5%)	
Female (%)	4832 (25.6%)	67 (61.5%)	
Height (M)	175.88 ± 6.97	177.97 ± 6.76	
(cm) (F)	163.63 ± 6.63	163.40 ± 5.56	
BMI (M)	N/A	26.70 ± 5.83	
(kg/m ²) (F)		23.28 ± 4.32	
Age (M)	N/A	36.79 ± 13.51	
(F)		38.27 ± 11.87	

Summaries are presented in mean ± SD.

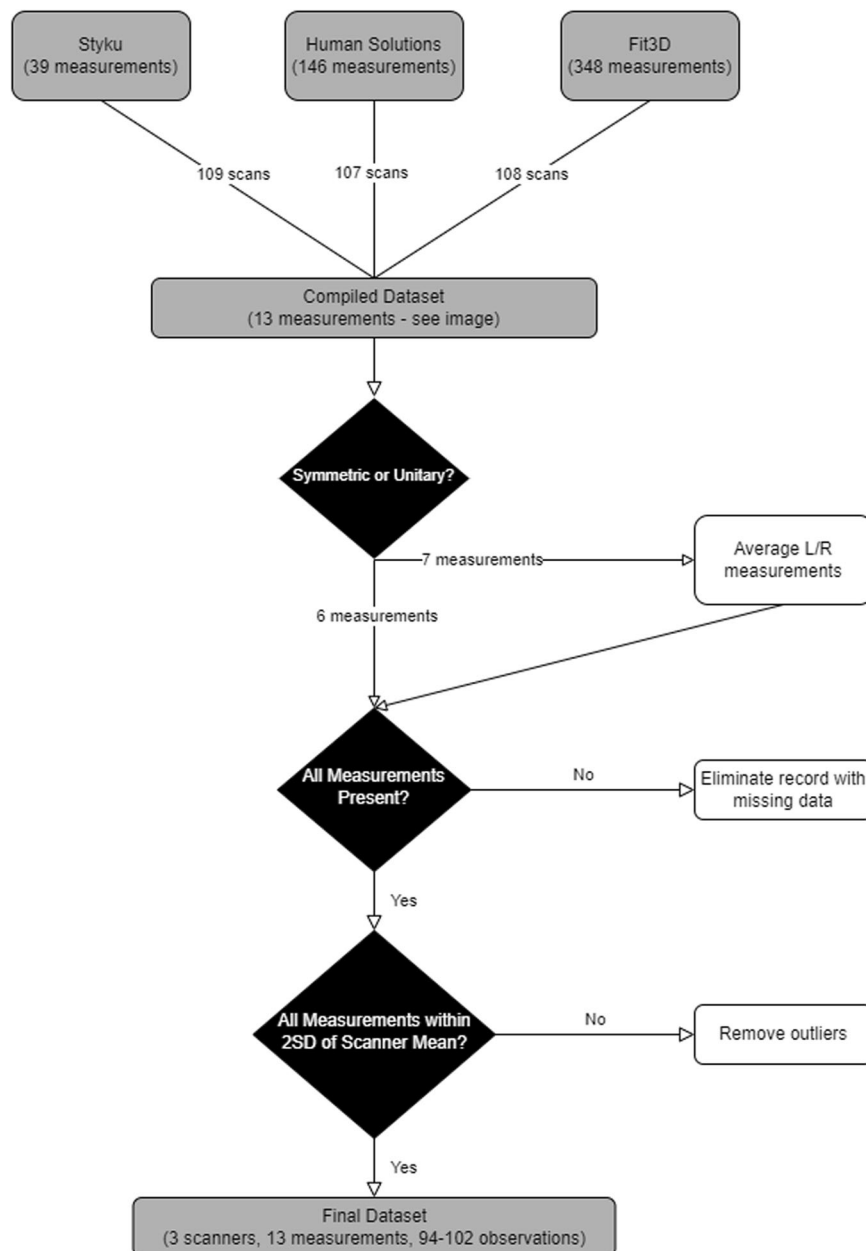


Fig. 1 Data preprocessing flowchart: symmetric body parts such as left and right bicep circumferences averaged. In pairwise midline comparisons, records with missing scanner data from an individual machine were eliminated. Outliers defined as measurements outside of 2 standard deviations from the mean.

positioning by a participant can render an implausible measurement which visually appears as an outlier. We quantified an outlier as any measurement at a body site two standard deviations away from the scanner measurements mean. Other studies have found such deviations were associated with invalid scans due to incorrect positioning by participants in the scanner [3, 9]. For all 13 anthropometric circumference sites, any data point outside this range resulted in removing the data point from the set. Before this step, the dataset contained 107 complete observations (13 measurements, 3 scanners, 107 observations). Using the method described above, we eliminated site specific values identified as outliers, with the remaining measurements detailed in Table 2.

Statistical methods

Regression models. Using Microsoft Excel, we developed a linear regression equation using explanatory variables from Fit3D or Styku measurements to the corresponding measurement in Human Solutions (Microsoft Excel O365, Seattle WA). Additionally, limits of agreement (Bland Altman [14]) analysis was performed and the bias and the 95% confidence interval were calculated.

Cluster analysis

Databases consisting of Styku measurements (West Point and Hawai'i) were converted to Human Solutions measurements using the developed regression models. We used these transformed datasets to compare variability through a k-means cluster analysis.

Circumferences	Body Site (L=Left, R=Right)
A	Bicep (L, R)
B	Lower Bicep (L, R)
C	Forearm (L, R)
D	Upper Thigh (L, R)
E	Mid-thigh (L, R)
F	Lower Thigh (L, R)
G	Calf (L, R)
H	Chest
I	Abdominal Waist
J	Narrowest Waist
K	Lower Waist
L	High Hip
M	Hip
N	Neck

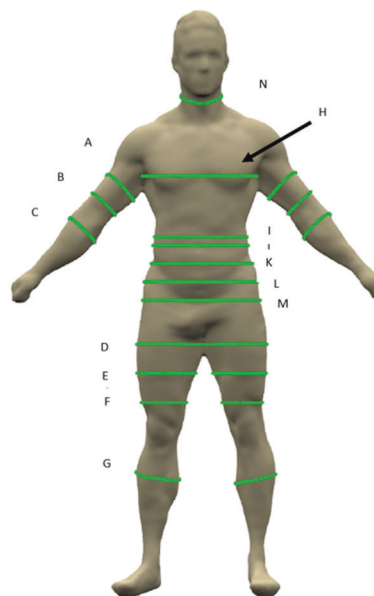


Fig. 2 An image of a Styku scanned avatar (on right) and circumferences that are output from the Styku scan device software. Once left and right circumference measurements were averaged a total of 13 measurements are available for analysis.

The k-means clustering algorithm [15] was performed with cluster numbers ranging from 2 to 19. A scree plot [15] was generated for each cluster analysis with the sum squared distance plotted on the y-axis and the number of clusters, k , plotted on the x-axis. The number of optimal clusters that describe the variance in the data was calculated as the number of clusters at the elbow of the scree plot.

The four datasets were pooled, and the cluster centroids (average value for each body scanner measurement) were calculated. A heat map was generated to visually display the degree of how much measurements in each clusters differ.

RESULTS

Linear regression conversion models

The number of complete observations applied for each regression model varied by body site and ranged from 94 observations to 100. Using each of the 13 anthropometric measurements as independent variables for each scanner yielded 39 regression equations. The equations appear in Table 2 along with the limits of agreement analysis (bias and 95% confidence interval). The weakest correlation between the Human Solutions and Styku occurred at the mid-thigh circumference site with an R^2 of 0.63. The strongest correlation between the Human Solutions and Fit3D occurred at the neck circumference site with an R^2 of 0.97. In general, Fit3D had better agreement with Human Solutions compared to Styku. The widest disagreement for both Fit3D and Styku occurred at the chest circumference measurement site. Compared to Human Solutions, Fit3D underestimated chest circumference (bias = 2.30, 95% CI = [-3.83, 8.43]) and Styku overestimated chest circumference (bias = -5.60, 95% CI = [-10.98, -0.22]).

Variability in body shapes detected through clustering

Figure 3 are scree plots describing the variability (y-axis) as cluster numbers increase (x-axis). The top left inset revealed the scree plot for the Hawai'i data, the top right showed the scree plot for the West Point data. The bottom left inset is the scree plot for the Lackland dataset and the bottom right is the scree plot for the Fort

Jackson data. The "elbow" for all scree plots occurred at approximately $k = 5$.

Although Fig. 1 in the Supplementary Materials shows that the elbow of the scree plot for the pooled data occurs around 5 clusters, we retained 6 clusters for inspection. Table 3 depicts the centroids of each measurement by cluster. The cluster labeled "D" consisted of individuals with substantially higher circumference measurements. For example, chest circumference was nearly double of all other clusters and mid-thigh circumference was approximately three times higher than the mid-thigh circumference means in the other clusters. Therefore, we did not include Cluster Number 4 in the heat map. Figure 4 depicts a heat map demonstrating how many standard deviations away each measurement value was from the mean of the remaining 5 clusters.

From the heat map (Fig. 4), Cluster 1 included taller males that had circumference measurements close to the overall averages. Cluster 2 consisted of tall males that had circumference measurements that were larger than average. Cluster 3 was 50% female and had smaller circumference measurements compared to the overall means. Cluster 5 were males that had measurements close to the mean.

DISCUSSION

In this study, we address the problem of combining and comparing data from popular commercially available 3D body scanners. There is a need to combine data to generate larger datasets or to compare across datasets that used different scanners. We demonstrate one example where 5 different clusters of body shapes were identified in a smaller restricted population of military cadets at the United States Military Academy at West Point. We needed to know if our findings generalize to a larger military population, however, in this smaller dataset, we are unable to extrapolate whether all US military personnel can be classified by 5 body shapes. Body scanner data existed, but unfortunately these measurements were not obtained using the same scanner. After developing regression models that translate

Table 2. Models that convert Fit3D and Styku to Human Solutions measurements.

Body Site	Neck	Chest	Biceps	Bicep Lower	Forearm	Waist (Narrowest)	Waist (Abdominal)	Waist (Lower)	High Hip	Upper Thigh	Mid-Thigh	Thigh Lower	Calf
N	94	100	96	100	99	99	99	100	102	98	99	101	98
Styku (regression model)	$y = 0.88x + 7.26$	$y = 1.06x - 0.01$	$y = 0.72x - 10.52$	$y = 0.83x + 6.26$	$y = 1.03x + 1.76$	$y = 1.11x + 0.99$	$y = 1.04x + 7.39$	$y = 1.04x - 1.29$	$y = 0.92x + 14.06$	$y = 0.68x + 18.18$	$y = 0.40x + 28.84$	$y = 0.55x + 15.57$	$y = 0.78x + 10.95$
Bias [95% CI]	-3.33 [-5.28, -1.37]	-5.6 [-10.98, -0.22]	-2.88 [-5.70, -0.07]	-2.09 [-4.42, 0.24]	-2.53 [-4.06, -1.01]	-8.85 [-12.85, -4.84]	-10.61 [-14.13, -7.10]	-1.73 [-8.66, 5.20]	-6.47 [-11.29, -1.65]	0.38 [-4.34, 5.10]	3.17 [-3.24, 9.57]	3.14 [-1.06, 7.33]	-3.37 [-6.17, -0.57]
R ²	0.95	0.93	0.82	0.80	0.91	0.96	0.95	0.81	0.86	0.77	0.63	0.70	0.70
Fit3D (regression model)	$y = 1.00x + 0.45$	$y = 0.9916x - 1.4691$	$y = 0.66x + 9.43$	$y = 0.94x + 2.29$	$y = 1.01x + 0.22$	$y = 0.98x + 3.42$	$y = 0.86x + 15.42$	$y = 1.12x - 15.26$	$y = 0.82x + 20.75$	$y = 1.00x + 0.33$	$y = 0.58x + 1.84$	$y = 0.96x + 1.43$	$y = 1.00x - 0.35$
Bias [95% CI]	-0.48 [-1.72, 0.76]	2.3 [-3.83, 8.43]	1.2 [-2.12, 4.52]	-0.73 [-2.3, 0.85]	-0.51 [-1.69, 0.67]	-1.99 [-8.72, 4.74]	-3.28 [-9.48, 2.91]	4.13 [-3.36, 11.62]	-2.54 [-8.19, 3.12]	-1.54 [-4.01, 0.92]	-1.61 [-5.57, 2.34]	-0.08 [-1.79, 1.64]	0.34 [-0.46, 1.14]
R ²	0.97	0.90	0.80	0.90	0.95	0.88	0.89	0.79	0.85	0.90	0.64	0.87	0.97

Formulation of the regression model, R² of the correlation plot, and the limits of agreement bias and 95% confidence interval are reported.

measurements from one scanner to another, we were able to re-run the analysis and answer this question in a larger database. The models presented here generalize to other applications that used different scanners and can be used to pool or compare across other datasets. The set of models presented in our study allows, for the first time, the combination of three scanner measurements after translating Fit3D and Styku measurements to Human Solutions standards.

Our study has several strengths. We maintain access to the only known dataset that contains simultaneous measurements with all three scanners in the same participants. Due to scanner expense and participant burden required for scanning and measuring multiple times, such a dataset proves rare and possibly unique. We also utilize to two smaller datasets of measurements obtained with Styku and two large datasets of Human Solutions scans obtained by the US Army at Fort Jackson and the US Air Force at Lackland. After standardizing all scanner data using the developed models, we compare findings across the datasets to classify archetype body shapes as a function of sample size.

Our study also has several limitations. First, including Styku distilled the feasible set of shared measurement sites to only 13, despite the wealth of numerous measurements output from Human Solutions and Fit3D. Second, the dataset used to translate measurements across the scanners arose from the PBRC study and had a small sample size. Despite these current limitations, our developed models offer the ability to extend into pooled data from other studies that do not suffer from the body composition restriction.

Why were only five clusters detected?

We expected to observe more clusters as the sample size increased. Löffler-Wirth et al. [16] found that increasing sample size resulted in approximately 15 clusters detected. The authors demonstrated the number of clusters increased with sample size and stabilized around 8000 participants. Our findings did not match those of Löffler-Wirth et al. [16] as we detected only 5 clusters even in the Lackland dataset which had over 24,482 observations. This mismatch possibly occurred since the larger datasets we applied consisted of a relatively homogenous population (i.e., military service members who must meet the body composition restrictions). Additionally, in the pooled cluster analysis, all the clusters except one were predominately male. While the Hawai'i dataset did not suffer from the same homogenous composition, the sample size consisted of only 527 participants. Of these participants, 131 formed a cluster that had substantially larger body circumferences in comparison to the others. The Hawai'i dataset matched the number of clusters detected by Löffler-Wirth et al. [16] at similar sample size. This observation suggests that with a more variable population, we would have had identified more archetype body shapes.

Pre-existing archetype body shapes from routinely collected anthropometry

Based on routinely collected circumferences (e.g. waist circumference and hip circumference), geometrical body shape characterizations have been classified. For example, when waist to hip ratio is 0.75 females are classified as pear shaped versus 0.82 where they are classified as apple shaped [17]. It has been well documented that apple shaped body types are at increased risk for metabolic and cardiovascular disease compared to pear shaped body types [18]. Combinations of these routinely collected anthropometric measurements have been developed into new indices to help classify shape and assess health and mortality risk [19]. However, these historical shape indices and classifications are restricted by the limited number of anthropometric measurements that are feasible to collect in a large sample.

Comparing Scree Plots

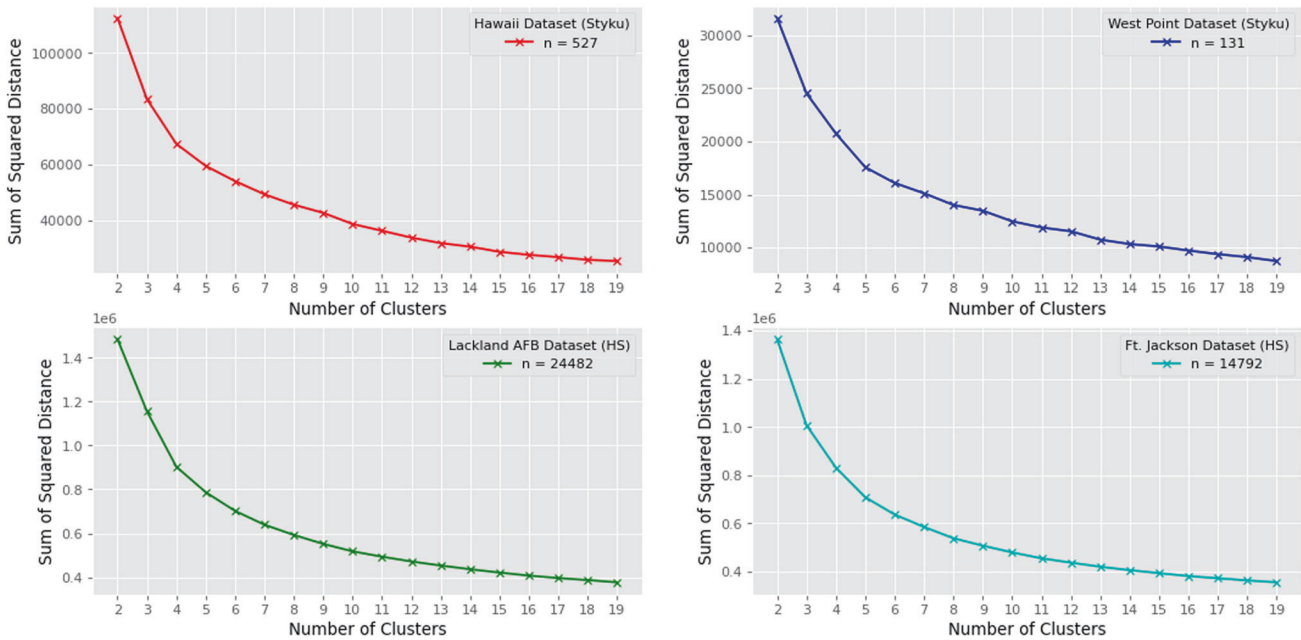


Fig. 3 Scree plots describing how much variability in body shapes were identified from the k-means cluster analysis. The top left inset is the scree plot representing the number of clusters for each dataset.

Table 3. Table depicting cluster centroids for the 6 clusters.

Cluster	N	%Males	Height	Neck	Chest	Biceps	Lower Bicep	Forearm
A	8576	0.99	181.56	14.74	38.56	11.79	10.53	10.32
B	6670	0.99	181.36	15.74	42.95	13.17	11.36	11.21
C	5636	0.48	161.21	13.57	36.44	11.01	9.63	9.39
D	131	0.65	174.74	13.94	93.82	29.27	25.75	25.41
E	9308	0.94	172.41	14.19	36.49	11.07	9.96	9.71
F	10,611	0.90	171.23	15.09	40.52	12.46	10.75	10.61
Cluster Number	Narrowest Waist	Abd. Waist	Lower Waist	High Hip	Upper Thigh	Mid Thigh	Lower Thigh	Calf
A	31.10	32.72	33.13	38.65	22.09	19.40	14.78	14.62
B	36.51	38.45	38.70	42.55	24.87	21.12	15.89	15.83
C	29.45	31.49	32.12	37.33	21.38	18.67	14.08	13.74
D	74.70	76.79	85.36	94.53	61.29	57.26	43.54	36.02
E	28.95	30.42	30.85	36.53	20.66	18.33	14.07	13.87
F	33.77	35.61	35.85	40.24	23.32	20.06	15.08	15.05

Cluster centroids are the cluster-specific mean values for each measurement.

Three-dimensional body shape scanners eliminate this restriction and reduce manual labor by capturing anywhere from dozens to hundreds of body site measurements within seconds. As we have demonstrated here, the high number of site measurements and the volume of scanned participants permits unsupervised machine learning through a cluster analysis. As opposed to defining thresholds that classify archetype shapes a priori, such as apple and pear shapes, clustering algorithms generate archetype body shapes derived from the data. For example, our study found 5 archetype body shapes that arose organically from the data. The newly identified archetype body shapes can then be used to predict outcomes of specific interest

such as pairing two datasets that used the same scanner [20], predicting debilitating injuries [3], and tracking body shape changes over the lifespan [21]. Such diverse and important applications that rely on 3D body shape anthropometry advance the original work that link lower numbers of archetype body shapes to metabolic and cardiovascular health outcomes [18].

CONCLUSIONS

Data obtained from different 3D body image scanners can be combined and compared after applying translating models that convert measurements between scanners. The ability to

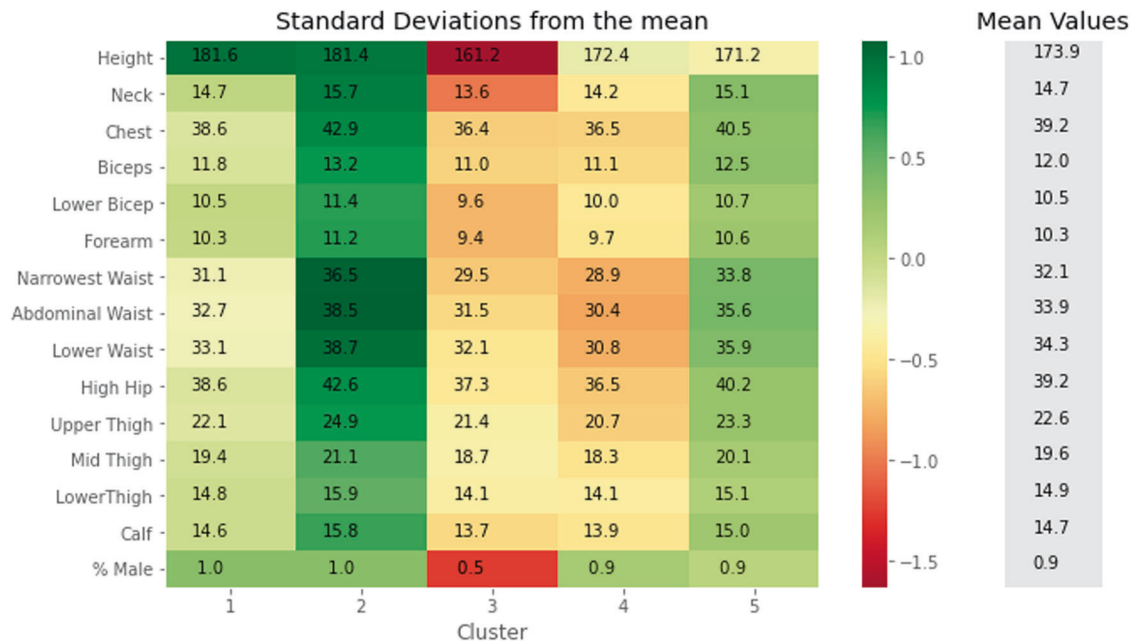


Fig. 4 Heat map of defined by standard deviations ranging from -1.5 to 1 away from the mean values of each measurement by cluster. Deeper red values signal measurements that are further left of the mean and more green values are measurements that are further to the right of the mean.

standardize measurements across scanners allows for sharing data across research sites and comparing and deriving meaningful conclusions.

DATA AVAILABILITY

Data will be made available by request after review by the United States Military Academy Chief Data Officer, Paul Evangelista. The review will determine the risks to personnel for data sharing and is dependent on the type of request. Requests can be made at paul.evangelista@westpoint.edu.

REFERENCES

- Istook CL 5 - Three-dimensional body scanning to improve fit. In: Fairhurst C (ed) *Advances in Apparel Production*. Woodhead Publishing, 2008, pp 94–116.
- Derouchey JD, Tomkinson GR, Rhoades JL, Fitzgerald JS. Reliability of the Styku 3D whole-body scanner for the assessment of body size in athletes. *Meas Phys Educ Exerc Sci*. 2020;24:228–34. <https://doi.org/10.1080/1091367X.2020.1791124>.
- Morse S, Talty K, Kuiper P, Scioletti M, Heymsfield SB, Atkinson RL, et al. Machine learning prediction of combat basic training injury from 3D body shape images. *PLoS One*. 2020;15:e0235017. <https://doi.org/10.1371/journal.pone.0235017>.
- Harty PS, Sieglinger B, Heymsfield SB, Shepherd JA, Bruner D, Stratton MT, et al. Novel body fat estimation using machine learning and 3-dimensional optical imaging. *Eur J Clin Nutr*. 2020;74:842–5. <https://doi.org/10.1038/s41430-020-0603-x>.
- Sobhiyeh S, Borel N, Dechenaud M, Graham CA, Wong M, Wolenski P, et al. Fully automated pipeline for body composition estimation from 3D optical scans using principal component analysis: a shape up study. *Annu Int Conf IEEE Eng Med Biol Soc IEEE Eng Med Biol Soc Annu Int Conf*. 2020;2020:1853–8. <https://doi.org/10.1109/embc44109.2020.9175211>.
- Bennett JP, Liu YE, Quon BK, Kelly NN, Leong LT, Wong MC, et al. Three-dimensional optical body shape and features improve prediction of metabolic disease risk in a diverse sample of adults. *Obes (Silver Spring, Md)*. 2022;30:1589–98. <https://doi.org/10.1002/oby.23470>.
- Sobhiyeh S, Kennedy S, Dunkel A, Dechenaud ME, Weston JA, Shepherd J, et al. Digital anthropometry for body circumference measurements: toward the development of universal three-dimensional optical system analysis software. *Obes Sci Pr*. 2021;7:35–44. <https://doi.org/10.1002/osp4.467>.
- Rhoades H. U.S. Army to evaluate relationship between body composition and physical fitness. *US Army*. 2021. <https://www.tradoc.army.mil/2021/10/19/u-s-army-to-evaluate-relationship-between-body-composition-and-physical-fitness/>.
- Watts K, Hwaung P, Grymes J, Cottam SH, Heymsfield SB, Thomas DM. Allometric models of adult regional body lengths and circumferences to height: insights from a three-dimensional body image scanner. *Am J Hum Biol: Off J Hum Biol Counc*. 2020;32:e23349. <https://doi.org/10.1002/ajhb.23349>.
- Tinsley GM, Moore ML, Dellinger JR, Adamson BT, Benavides ML. Digital anthropometry via three-dimensional optical scanning: evaluation of four commercially available systems. *Eur J Clin Nutr*. 2020;74:1054–64. <https://doi.org/10.1038/s41430-019-0526-6>.
- Heymsfield SB, Smith B, Wong M, Bennett J, Ebbeling C, Wong JMW, et al. Multicomponent density models for body composition: Review of the dual energy X-ray absorptiometry volume approach. *Obes Rev*. 2021;22:e13274. <https://doi.org/10.1111/obr.13274>.
- Bennett JP, Liu YE, Quon BK, Kelly NN, Wong MC, Kennedy SF, et al. Assessment of clinical measures of total and regional body composition from a commercial 3-dimensional optical body scanner. *Clin Nutr (Edinb, Scotl)*. 2022;41:211–8. <https://doi.org/10.1016/j.clnu.2021.11.031>.
- Thomas DM, Galbreath D, Boucher M, Watts K. Revisiting Leonardo da Vinci's Vitruvian man using contemporary measurements. *Jama*. 2020;323:2342–3. <https://doi.org/10.1001/jama.2020.3501>.
- Bland JM, Altman DG. Measuring agreement in method comparison studies. *Stat Methods Med Res*. 1999;8:135–60. <https://doi.org/10.1177/09622802990800204>.
- James G. An introduction to statistical learning with applications in R. In: Witten D, Hastie T, Tibshirani R, (eds). 2nd ed. ed. New York: Springer %J Springer Texts in Statistics Ser. 2021. https://books.google.com/books/about/An_Introduction_to_Statistical_Learning.html?id=qc_AAAAQBAJ.
- Löffler-Wirth H, Willscher E, Ahnert P, Wirkner K, Engel C, Loeffler M, et al. Novel anthropometry based on 3D-bodyscans applied to a large population based cohort. *PLoS One*. 2016;11:e0159887. <https://doi.org/10.1371/journal.pone.0159887>.
- Thoma ME, Hediger ML, Sundaram R, Stanford JB, Peterson CM, Croughan MS, et al. Comparing apples and pears: women's perceptions of their body size and shape. *J Women's Health (Larchmt)*. 2012;21:1074–81. <https://doi.org/10.1089/jwh.2012.3634>.
- Lebovitz HE. The relationship of obesity to the metabolic syndrome. *Int J Clin Pract*. 2003; 18–27. <https://pubmed.ncbi.nlm.nih.gov/12793594/>.
- Maessen MF, Eijssvogels TM, Verheggen RJ, Hopman MT, Verbeek AL, de Vegt F. Entering a new era of body indices: the feasibility of a body shape index and body roundness index to identify cardiovascular health status. *PLoS One*. 2014;9:e107212. <https://doi.org/10.1371/journal.pone.0107212>.
- Pleuss JD, Talty K, Morse S, Kuiper P, Scioletti M, Heymsfield SB, et al. A machine learning approach relating 3D body scans to body composition in humans. *Eur J Clin Nutr*. 2019;73:200–8. <https://doi.org/10.1038/s41430-018-0337-1>.
- Frenzel A, Binder H, Walter N, Wirkner K, Loeffler M, Loeffler-Wirth H. The aging human body shape. *NPJ Aging Mech Dis*. 2020;6:5 <https://doi.org/10.1038/s41514-020-0043-9>.

AUTHOR CONTRIBUTIONS

DMT, MS, MM, and NA conceived this study. JS, NG and SBH provided data and data interpretation for this study. NA performed the statistical analysis under supervision from DMT, MS, and DR. DMT and NA prepared the first draft of the manuscript. MM, BB, and BAS provided insight into US Army problems with different scanners. All authors reviewed multiple drafts of the manuscript.

FUNDING

MS and DMT were funded by NIH U54TR004279.

COMPETING INTERESTS

The US Military Academy has no affiliation with any industry and DMT, NA, DR, and MS have no conflicts of interest or financial disclosures. also have no conflicts of interest or financial disclosures. JS has an investigator initiated grant with Hologic. JS is on the scientific advisory board for Styku and Hologic. JS has some stock options

for being on the boards of Styku and formerly on BodySpec (value < \$10k). Steven B. Heymsfield reports his role on the Medical Advisory Boards of Tanita Corporation, Amgen, and Medifast; he is also an Amazon Scholar.

ADDITIONAL INFORMATION

Supplementary information The online version contains supplementary material available at <https://doi.org/10.1038/s41430-023-01289-5>.

Correspondence and requests for materials should be addressed to Diana M. Thomas.

Reprints and permission information is available at <http://www.nature.com/reprints>

Publisher's note Springer Nature remains neutral with regard to jurisdictional claims in published maps and institutional affiliations.